Spatial Localization of Cancer Cell Intravasation to the Interior Core of Primary Tumor Independent of Invasion into Adjacent Stroma

Elena I. Deryugina and William B. Kiosses

Supplemental Experimental Procedures

Syngeneic mouse ear tumor model

C57Bl/6J mice were obtained from The Jackson Laboratory and maintained at TSRI under established animal protocols. Murine melanoma B16F10 was purchased form ATCC. For primary tumor formation, ~5 µL of B16F10 cell suspension ($1x10^7$ cells/mL) were inoculated into the ear dermis of syngeneic C57Bl/6J mice (**Figure S1**) essentially as described (Hirayama et al., 1984). Visible tumors are generated within 6-9 days (**Figure S1A)** and by day 13-14 primary tumors are fully formed (**Figure S1B***i*) and tumor-bearing mice demonstrate metastasis into the cervical lymph nodes (**Figure S1B***ii*). If the primary tumor is removed, the mice within 2 weeks present with metastases in the inguinal lymph nodes (**Figure S1B***iii*) and lungs (**Figure S1B***iv*). Importantly, the primary ear tumors are highly vascularized, displaying a well-developed network of angiogenic vessels (**Figure S1C**).

Chick embryo spontaneous intravasation and metastasis model

Spontaneous dissemination of tumor cell to the CAM vasculature was analyzed also for primary tumors generated in chick embryos developing *in ovo* (Bekes et al., 2011b; Deryugina et al., 2005). Tumor cells were placed on the top of the CAM ($5x10^5$ per embryo) and 5 days later, the portions of distal CAM were removed and analyzed by *Alu*-qPCR to determine actual numbers of human tumor cells that spontaneously entered the CAM vasculature (intravasation) (Bekes et al., 2011a; Conn et al., 2009; Deryugina et al., 2005; Juncker-Jensen et al., 2013).

siRNA transfections

Pools of 3 to 5 small interfering RNA (siRNA) against human EGFR (siEGFR; sc-29301), GFP (siGFP; sc-45924), and non-silencing control siRNA (siCtrl; sc-37007) were purchased form Santa Cruz. The day before transfections, the HT-hi/diss and HEp3 cells were plated in serum-containing medium without antibiotics at concentrations resulting in 70-80% confluence the following day. Transfections were performed with 50 nM siRNA and Lipofectamine 2000 or RNAiMax (Life Technologies), according to

the manufacturer's instructions. After an overnight incubation, the siRNA-treated cells were detached, washed in D-10 and SF-DMEM, re-suspended in SF-DMEM, and used in the various assays. The levels of EGFR expression were verified by western blot analysis.

Western blot analysis

Expression of EGFR was analyzed in tumors cells 4-5 days after cell transfections with siCtrl or siEGFR. Tumor cells were washed and lysed in mRIPA buffer. Equal amounts of protein (20 µg per lane) were reduced, separated in 4-20% Tris-glycine SDS-PAGE gels (Life Technologies), and transferred to a PDVF membrane (Immobilon). After blocking with 5% milk in PBS/0.05% Tween 20, the membranes were incubated overnight with rabbit antibody against EGFR (2646 from Cell Signaling Technology) or mouse α-tubulin antibody 10D8 (BioLegend) at 1 µg/ml in 5% milk in PBS/0.05% Tween 20. After washing, the membranes were incubated with corresponding secondary HRP-conjugated goat anti-rabbit antibody 7074 or horse anti-mouse antibody 7076 (both from Cell Signaling), used at 1:5,000 for 1 hr at room temperature. Immunoreactive bands were visualized using SuperSignal West Pico Chemiluminescent Substrate (Pierce).

Quantitative PCR to detect human-specific Alu repeats (Alu-qPCR)

Quantification of human tumor cells disseminated in mouse or chick embryo models was performed with quantitative real time PCR assay originally established in L. Ossowski laboratory (Kim et al., 1998) and successfully used by us with some modifications (Bekes et al., 2011b; Conn et al., 2009; Deryugina et al., 2005; Juncker-Jensen et al., 2013; Zijlstra et al., 2002). This assay is based on the quantification of human-specific *Alu* sequence repeats in total DNA extracted from the host tissue. Briefly, genomic DNA was extracted from the CAM tissue using the Puregene DNA purification system (Qiagen, Minneapolis, MN). *Alu*-qPCR was performed to amplify primate-specific *Alu* repeat sequences using 10 ng of genomic DNA as a template in a Bio-Rad MyIQLightCycler (Bio-Rad, Hercules, CA). The dsDNA binding dye SYBR green (Life technologies, Grand Island, NY) was used for quantification of human tumor cells. The cycle threshold (*C*t) values were converted into numbers of human cells using a standard curve generated by spiking constant numbers of chicken cells with serially diluted human tumor cells.

Quantification of vasculotropism in vivo

Vasculotropic invasion was measured in epifluorescent images, as maximal distance traveled by tumor cells from the edge of a primary tumor along tumor-coalescing blood vessels. Up to 10 measurements

were conducted for each individual tumor in 3-4 independent experiments. Vasculotropic cells were identified as tumor cells aligned along blood vessels and localized at less than 5 μm distance from the abluminal vessel surface and quantified as the percentage of vasculotropic tumor cells relative to all escaped tumor cells outside of the primary tumor border.

Measurement of vasculature permeability in vivo in tumor-bearing embryos

CAM primary tumors were initiated from non-labeled HT-hi/diss tumor cells to allow for subsequent use of the permeable, low mol. wt. TRITC-conjugated "red" dextran and non-permeable, high mol. wt. FITC-conjugated "green" dextran (155 kDa and 2,000 kDa, respectively; both from Sigma). On day 5 after tumor cell grafting, tumor-bearing embryos were first inoculated with the permeable red dextran and after 1 hr incubation (allowing for dextran leakage), the embryos were inoculated with non-permeable green dextran, allowing to highlight the vascular bed in both intratumoral and tumor-adjacent regions of the CAM. After a short, 10-min incubation, the portions of the CAM containing primary tumors along with adjacent areas were excised and imaged at low magnification in an Olympus immunofluorescent microscope equipped with the 2x and 4x objectives and a video camera. The images were acquired monochromatically in green and red channels and saved using Pictureframe software. The acquired images were quantitatively analyzed with the ImageJ program for the intensity of red fluorescence (representing the leaked dextran) in the interior of the tumor *vs.* the areas adjacent to the tumor border. The green fluorescence (representing the perfusable vasculature) was measured in the same areas, allowing to quantify the permeability indices in the individual areas of tumor-containing portions of the CAM, i.e. the ratio between the levels of red dextran exudation *vs.* the total volume vessels containing non-permeable green dextran. The difference between permeability indices for the tumor core and tumor-adjacent areas was statistically evaluated by the paired two-tailed Student *t*-test for $P<0.05$.

Measurement of hypoxia in vivo in tumor-bearing embryos

Levels of hypoxia *in vivo* in different areas of primary tumors were measured with pimonidazole, a bioreductive chemical probe that forms protein adducts in viable hypoxic cells, where pO_2 is less than 10-20 mmHg (Li et al., 2007; Rademakers et al., 2011). Intramesodermal tumors were initiated from GFP-labeled HT-hi/diss or Hep3 cells. On day 5 (HT-hi/diss) or 7 (HEp3) after tumor cell grafting, tumor-bearing embryos were inoculated i.v. with a solution pimonidazole hydrochloride (Hypoxyprobe Inc., Burlington, MA) at 7.5 mg per embryo in 0.2 ml PBS. Embryos were incubated for 2 hr, allowing for the formation of pimonidazole adducts. At the end of incubation, the embryos were injected with 0.15-0.2 ml of DyLight 649-conjugated LCA (Vector Laboratories) to highlight the vasculature. Following 10-15 min

incubation, the portions of the CAM containing primary tumors and tumor-adjacent areas were fixed in Zn-buffered 10% formalin (Company). After overnight fixation, tissue samples were washed in PBS and permeabilized in 1% Triton X-100 for 2 hrs at room temperature or overnight at 4^0C. After blocking with 10% goat serum in PBS supplemented with 5% BSA and 0.1% Triton X-100, tissue samples were stained for 2 hr at room temperature or overnight at 4^0C with the DyLight 549-conjugated mouse anti-pimonidazole antibody 4.3.11.3 (Hypoxyprobe Inc.), used at 20 µg/ml in PBS supplemented with 0.1% BSA and 0.1% Triton X-100. After washing in PBS, tissue samples were imaged monochromatically in green, red and far-red channels using an Olympus immunofluorescent microscope (Olympus) equipped with the video camera and Pictureframe software. Acquired imaged then were analyzed and quantified using ImageJ software and then, monochromatic images were colored and merged using Adobe Photoshop.

Since CAM tissue is highly oxygenated (the pO_2 levels in blood of chick embryos are ~ 50 mmHg), for positive control hypoxia was induced *in vivo* by treating tumor-bearing embryos with the hypoxia mimetic agent $CoCl_2$ (Bauer et al., 2014). Cobalt chloride solution (100 mM in PBS supplemented with 5% DMSO) or vehicle was applied topically at 0.1 ml over a primary tumor (not more than 0.5 ml of $CoCl_2$ solution per embryo). Embryos were incubated for 1 hr to allow for generation of oxygen-deprived areas containing primary tumors. Then pre-treated embryos were inoculated with pimonidazole and tissue samples harvested and processed for immunofluorescent microscopy as described above.

In vivo detection of EGFR activity in primary tumors

To detect the activity of EGFR in vivo, intramesodermal CAM tumors were initiated from GFP-labeled HT-hi/diss or HEp3 cells. On day 5 and 7, correspondingly, the portions of the CAM containing primary tumors were excised from tumor-bearing embryos and fixed in Zn-buffered 10% formalin. After overnight fixation, tissue samples were washed in PBS and permeabilized in 1% Triton X-100 for 2 hrs at room temperature or overnight at 4^0C. After blocking with 10% goat serum in PBS supplemented with 5% BSA and 0.1% Triton X-100, tissue samples were stained overnight at 4^0C with mouse monoclonal antibodies against phosphorylated EGFR (pEGFR), F9 (HT-hi/diss) or E8 (Hep3) (both from Santa Cruz), diluted at 20 µg/ml of PBS supplemented with 0.1% BSA and 0.1% Triton X-100. After washing with PBS, tissue samples were additionally stained with 20 µg/ml of rabbit antibody 2646 against EGFR (total EGFR) (Cell Signaling) in PBS supplemented with 0.1% BSA and 0.1% Triton X-100. After washes in PBS, tissue samples were incubated for 2 hr at room temperature with the mixture of goat anti-mouse antibody conjugated with Alexa Fluor 546 (Molecular Probes) and donkey anti-rabbit antibody

conjugated with DyLight 594 (BioLegend). After extensive washing in PBS, tissue samples imaged monochromatically in green, red and far-red channels using an Olympus immunofluorescent microscope. Images were acquired monochromatically and then, combined and merged using Adobe Photoshop.

Ex vivo model to measure tumor cell vasculotropism

Vasculotropic behavior of tumor cells was measured in our modification of a Transwell model. The porous 8 um-pore membrane of 6.5-mm inserts was occluded with native fibrillar type I collagen (2 ug per membrane) to provide a 3D barrier for invading tumor cells. Venous blood vessels were excised from the CAM of day 12-15 chick embryos, washed of blood, and cut into ~0.5 mm pieces. Five to six vessel pieces were distributed in the wells of the 24-well plate pre-filled with 0.5 mL of 2.5 mg/mL collagen solution, which was then allowed to solidify at 37^{o}C and overlaid with serum-free DMEM (SF-DMEM; 0.5 mL/well). Collagen-occluded Transwell inserts were filled with 1x10^{5} GFP-tagged tumor cells in 0.1 mL SF-DMEM and placed into the wells containing blood vessels within 3D collagen gels. After 48 hours, GFP-positive tumor cells that migrated through the collagen barrier were recovered from the outer chamber and cells quantified in an epifluorescent microscope.

Acquisition and image analysis for quantification of tumor cell intravasation

The z-series images of primary tumors, containing GFP-tagged tumor cells and the vasculature highlighted *in vivo* with a red fluorescent dye, were acquired with a Zeiss LSM 780 Laser scanning confocal microscope (Zeiss Inc) using either a 20x- or 40x objective (**Figure S2a).** The auto-tiled images were stitched with a 10% overlap using the multi-tiling software module in ZEN to create a 3D mega image of the whole tumor region, which would allow its analysis as an entire unit. The final mega images were imported into IMARIS as raw ZEN czi files, retaining all original meta data. The surface rendering (isosurfacing) and MATlab macros were used within IMARIS (**Figure S2b**), to develop two distinct intravasation-scoring approaches to define the proximity of the tumor cells to the center of a nearest vessel and to determine whether a tumor cell is localized completely within the vessel wall. Both scoring methods involve thresholding the original signal for the vasculature to create a 3D-rendered tubular isosurface. This process was performed twice: first time, to follow and outline the exterior of blood vessels (**Figure S2c**), and second time, to fill in (solidify) the tubular structures (**Figure S2d**), allowing us to establish (score) a point of reference for tumor cells adjacent to the vessels.

In the first, ***IMARIS mapping*** method for scoring of intravasation events (**Figures S2e and S2f**), a distance transform module was used to define mathematically the distance (in μm) between each tumor cell surface facing the nearest vessel and the center of the vessel lumen. Using a spectral "***violet-to-red"***

table (presented at the bottom of **Figure S2**), all tumor cells within the primary tumor were color-coded in accordance to their distance to the center of the lumen of an adjacent and nearest vessel. Tumor cells located within 2 µm from the center of a proximal vessel were defined as red-orange ("***hot***") in the color map. Correspondingly, the "*hot*" tumor cells would comprise tumor cells fully positioned within the lumen (intravasated) as well as a population of tumor cells that penetrate the vessel wall (intravasating). The majority of these "*hot*" cells (**Figure S2e**) become "invisible" when viewed along with the IMARIS-rendered solidified 3D vasculature (**Figure S2f**), confirming their true intravascular position.

The second, ***IMARIS mask*** intravasation-scoring method delineates more specifically the fully intravascular-positioned tumor cells (**Figure S5**). Similar to the first approach, the original "vasculature" fluorescent signal (**Figure S5a**), was imported into IMARIS to create an isosurface-rendered tubular reconstruction of the vasculature that was first outlined and then, masked and solidified (**Figure S5b**). By creating a solid 3D mask of the vessel luminal space, this approach allows us to extract any and all green signals (tumor cells) "trapped" within the mask or colocalized with the red fluorescence vascular signal. By applying more stringent criteria such as signal intensity and size/volume of objects, the tumor cells that are on the vessel surface or partially entering into the blood vessel are distinguished and excluded from those tumor cells that are entirely within the lumen. The translucent mode allows to visualize these truly intravascular tumor cells (**Figure S5c**), since they become absent from the view when the vessel surface is made opaque (**Figure S5d).** These fully intravasated tumor cells can now be segregated ("extracted") as a distinct cell population (**Figure S5e**) from the entire population of primary tumor cells (**Figure S5f**), that usually are too dense to allow for reliable and unbiased discrimination between their intraluminal or abluminal positions (**Figure S5g**). The side view on cross-sections presents an example validating that each and all tumor cells that are "extracted" by our stringent intravasation-scoring method are truly intravascular, i.e. actual intravasated tumor cells (**Figure S5, h-j**). Thus, when vessel luminal space has been solidified (**Figure S5h**), tumor cells within vessels are visible in a translucent mode (**Figure S5i**) and disappear when the vessel surface made opaque except for the cross section (**Figure S5j**).

Our two novel intravasation-scoring methods provide similar quantitative data for intravasated/intravasating tumor cells, the latter allowing to quantify exclusively tumor cells fully positioned within the vessel lumen, that is, intravasated tumor cells; and the former comprising both intravasating and intravasated cells. Furthermore, since the first method does not distinguish the intravasating cells from extravasating cells (remote, but a possibility), the second, more stringent method is considered as the more definitive for quantification of tumor cell intravasation.

Supplemental Data

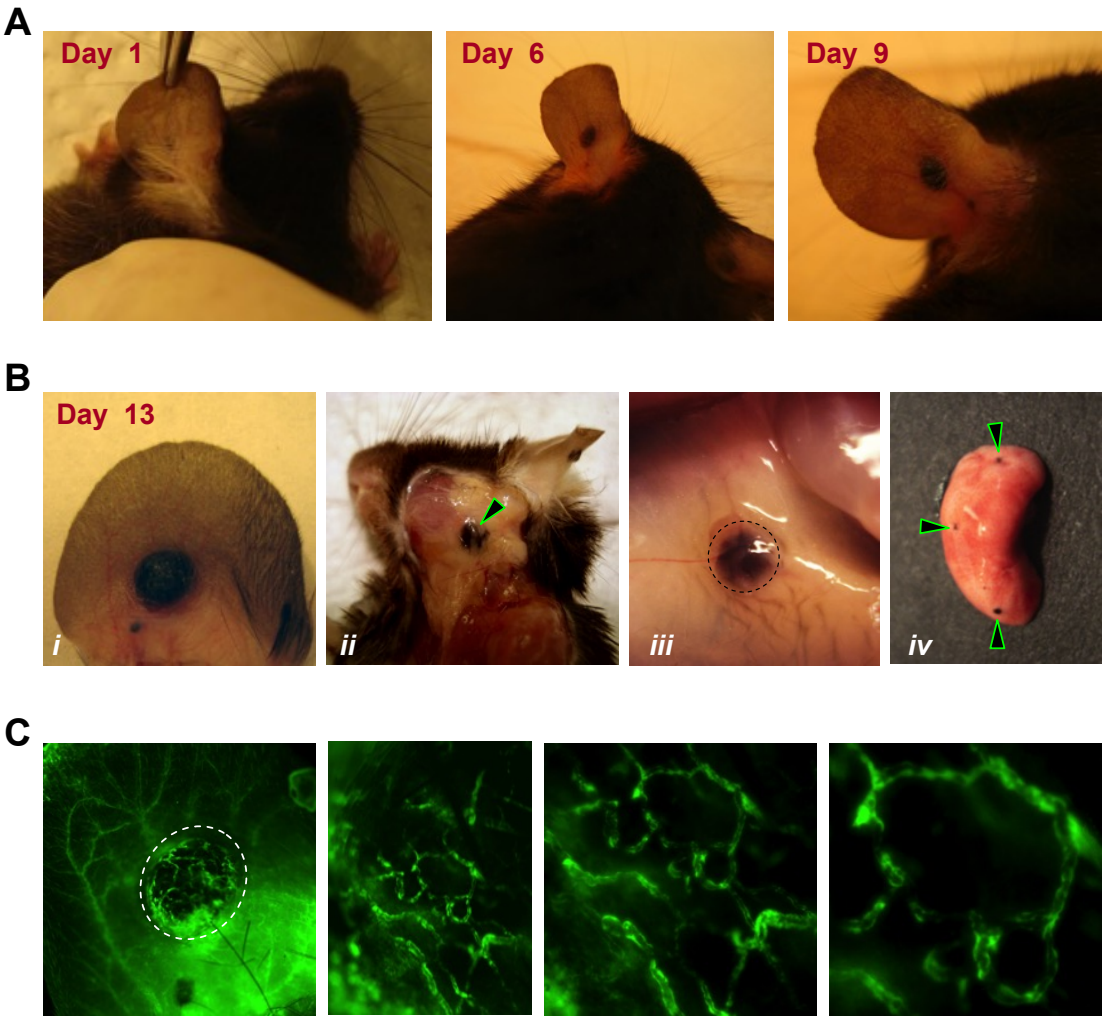

Figure S1 related to Figure 1. Syngeneic mouse ear tumor model.

Murine B16F10 melanoma cells were implanted intradermally into C57BL/6 mice. Visible tumors are generated within 6-9 days (**A**). By day 13-14, primary tumors are fully formed **(B*i*)** and the tumor-bearing mice demonstrate metastasis into local cervical lymph nodes **(**arrowhead in **B*ii*)**. If the primary tumor is removed, the mice within 2 weeks present with metastases in the inguinal lymph nodes **(**dotted line in **B*iii*)** and lungs **(**arrowheads in **B*iv*)**. Importantly, the primary ear tumors are highly vascularized, displaying a well-developed network of angiogenic vessels highlighted in (**C**) with i.v.-inoculated FITC-conjugated dextran.

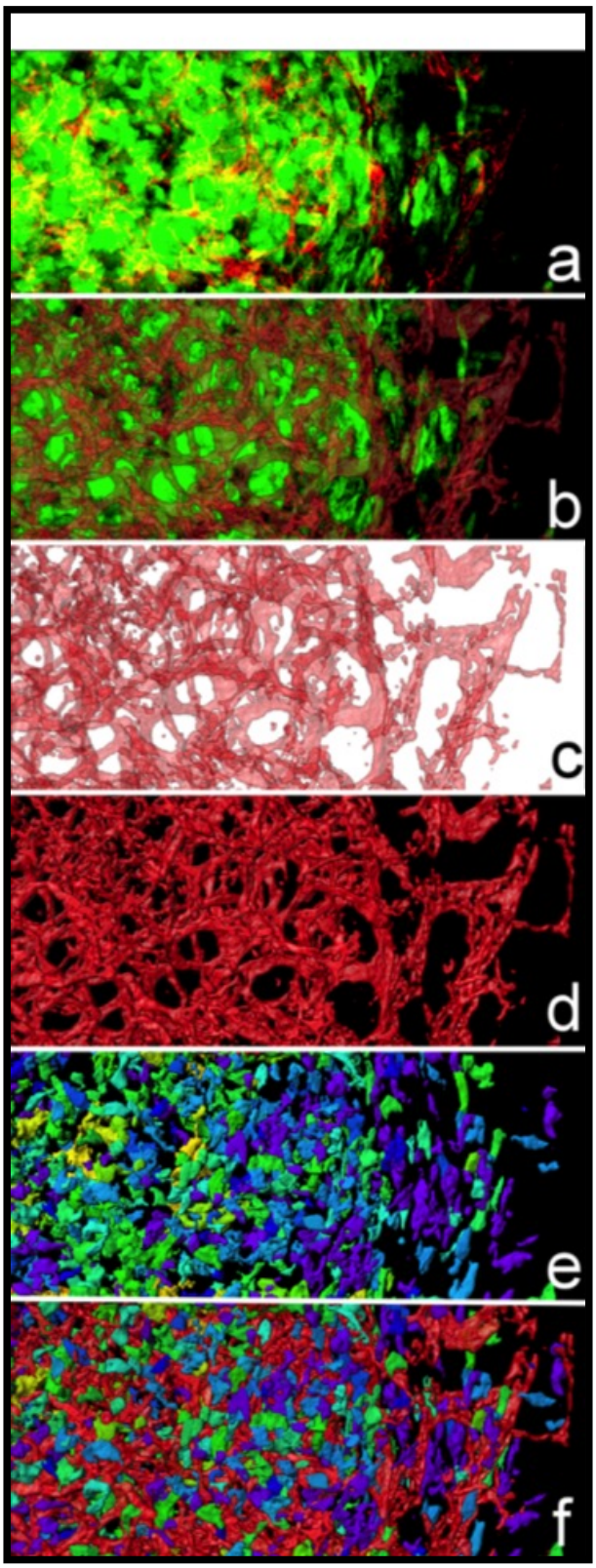

Figure S2 related to Figure 4.

Scoring of tumor cell intravasation within the primary tumor by "cell mapping" method.

Figure depicts a sequence of steps conducted within the first intravasation-scoring method used to create a distance transform map that determines the position of tumor cells relative to the lumen center of the nearest blood vessel. The steps are described in more detail in the corresponding section on pages 3-4.

(a) original image with the signals for tumor cells (*green*) and vasculature (*red*) merged;

(b) IMARIS-rendered isosurfaced vasculature and tumor cells;

(c) IMARIS-rendered isosurfaced vasculature only;

(d) 3D-solidified vessel lumen space following second round of IMARIS isosurfacing;

(e) Distance transform map of primary tumor cells. Based on the coldor scale indicated at the bottom of the figure, tumor cells are ranked (colored) depending on their distance from the lumen center of the nearest vessel: the yellow-orange-red cells ("*hot*") assigned as being inside the vasculature or crossing the vessel wall ("*in lumen*").

(f) Color-coded tumor cells (**e**) visualized simultaneously with the IMARIS-rendered solidified 3D vasculature (**d**). Note that the majority of "*hot*" cells become "invisible" when viewed along with solidified red-colored vasculature.

Color scale at the bottom is used to "color code" primary tumor cells depending on their distance from the center of the nearest vessel lumen.

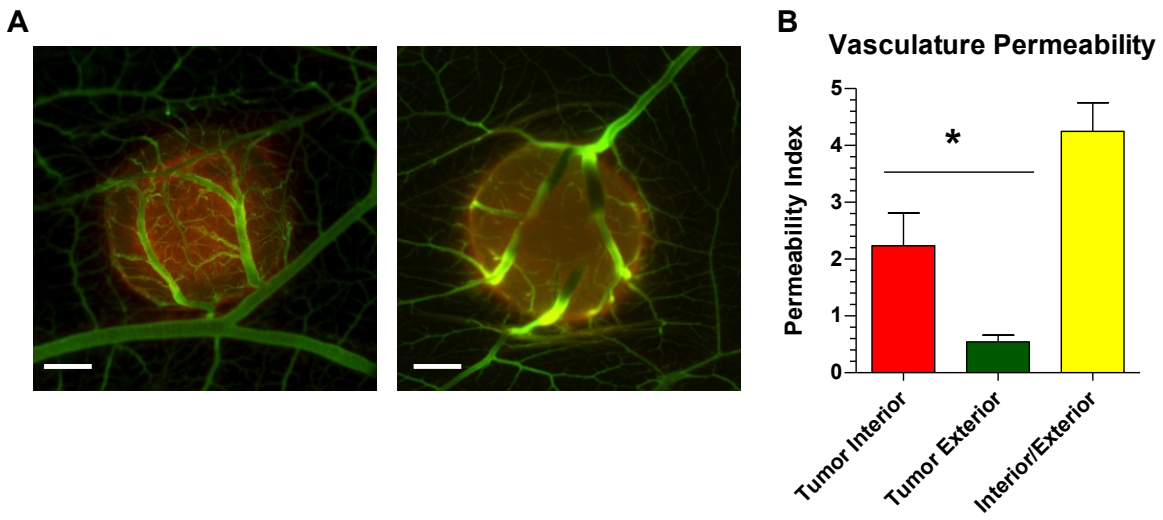

Figure S3 Related to Figure 4. Spatial analysis of the permeability of the vasculature within the core of primary tumors *vs.* tumor-adjacent blood vessels.

(A) CAM primary tumors were initiated from non-labeled HT-hi/diss tumor cells. On day 5 after tumor cell grafting, tumor-bearing embryos were first inoculated with the permeable "red" dextran and after 1 hr incubation (allowing for dextran leakage), the embryos were inoculated with non-permeable "green" dextran to highlight the vascular bed in both intratumoral and tumor-adjacent regions of the CAM. After a short, 10-min incubation, the portions of the CAM containing primary tumors along with tumor-adjacent areas were excised and imaged at low magnification in a immunofluorescent microscope. The representative images illustrate that dextran exudation occurs mainly within the tumor core, indicating that the intratumoral vessels are leaky. Scale bars, 500 μm.

(B) The images acquired monochromatically in red and green channels were quantitatively analyzed for the intensity of red fluorescence (representing the leaked dextran) in the tumor core area *vs.* the area adjacent to the tumor border. The green fluorescence was measured in the same areas, allowing to quantify the permeability indices, i.e. the ratios between the levels of red dextran exudation *vs.* the volume of perfusable vessels containing non-permeable green dextran. This differential analysis confirms that dextran exudation occurs mainly within the tumor interior and indicates that the permeability index is more than 4-fold higher for the intratumoral vasculature than for tumor-adjacent vessels ($P<0.05$; n=11; 2 independent experiments).

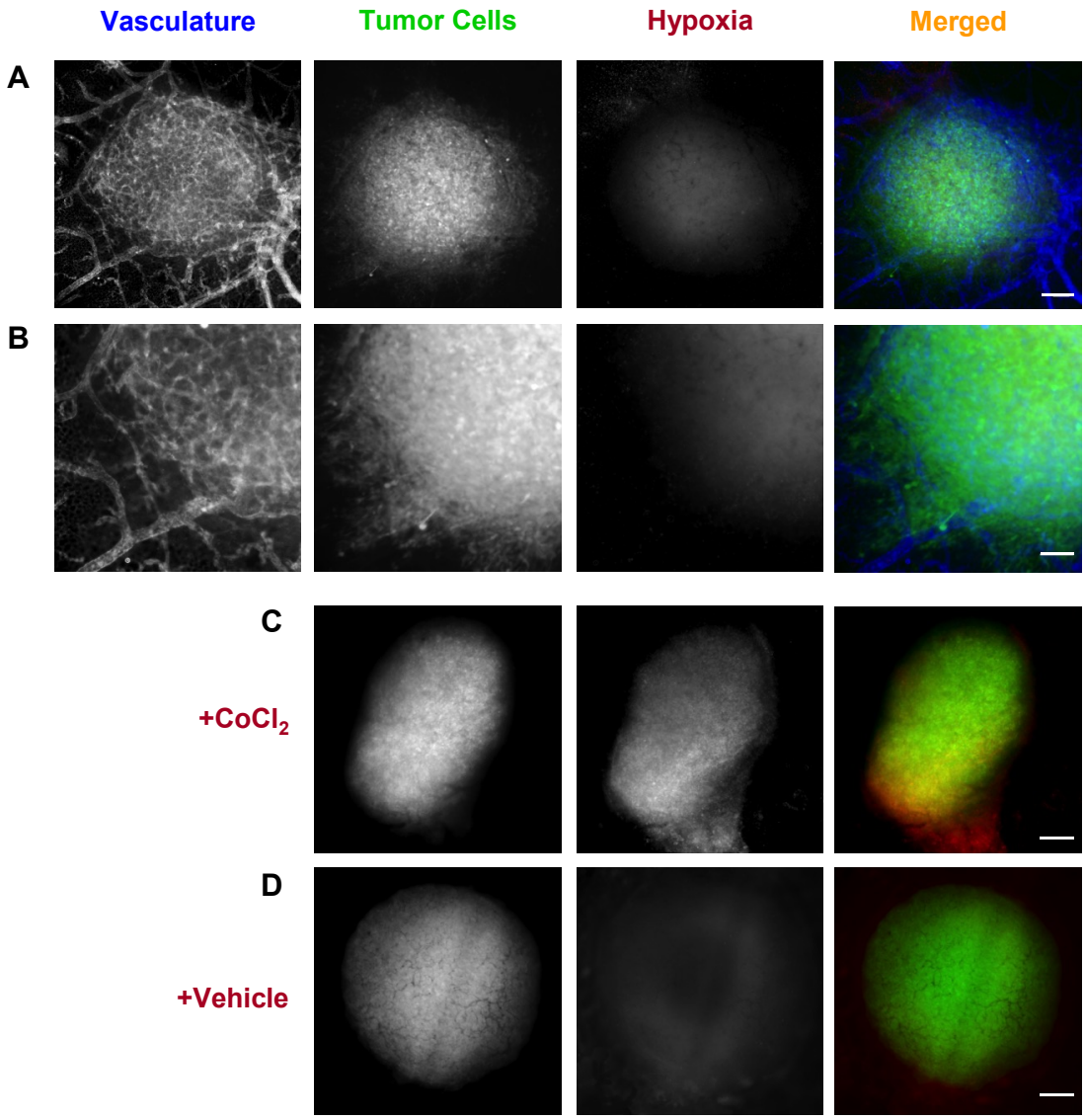

Figure S4 Related to Figure 4. ***In vivo*** **analysis of hypoxia levels in primary CAM tumors.** Intramesodermal tumors were initiated from GFP-HT-hi/diss cells (**green**). On day 5 after tumor cell grafting, tumor-bearing embryos were inoculated with the hypoxia probe pimonidazole. The formed protein adducts were detected with anti-pimonidazole-specific antibody (**red**). The vasculature was highlighted *in vivo* with the far-red DyLight 649-conjugated LCA (depicted in **blue**).

(A and B) Analysis of hypoxia in different portions of primary tumors. Representative HT-hi/diss primary tumor along with tumor-adjacent areas with invasive outgrowths was imaged at the 10x objective (**A**). Scale bar, 200 µm. The lower left quadrant of the tissue sample depicted in A was imaged at 20x

magnification in (**B**), to simultaneously present the portion of tumor core and stroma-invasive tumor outgrowths along tumor-coalescing blood vessels. Scale bar, 100 μm.

In agreement with high levels of neovascularization of primary tumors, the above presented staining indicates overall very low levels of hypoxia in the primary tumor core: The low levels of hypoxia were detected only in the most inner portion of the tumor core. Importantly, these levels of hypoxia were comparable with the levels of hypoxia observed in the embryos that did not receive any pimonidazole (data not shown). Furthermore, the areas of invasive tumor outgrowths into tumor-adjacent stroma along blood vessels (areas to the left and bottom in the B panels) appear completely negative for hypoxia, consistent with high levels of oxygenation provided by CAM vasculature.

(C and D) Induction of hypoxia in tumor-bearing embryos. As a positive control for hypoxia detection with the pimonidazole probe, primary tumors were treated with a solution of $CoCl_2$ to induce local hypoxia *in vivo* (**C**) or treated with vehicle (**D**). Hypoxia (red in the merged panels on the right) was detected as described above in the experimental procedures. Scale bars, 200 μm.

Note, that the oxygen-depriving agent, $CoCl_2$, applied topically to the area of the primary tumor, induced high levels of hypoxia. In contrast, negligible levels of hypoxia were observed in vehicle-treated control embryos, consistent with high levels of neovascularization and oxygenation within the core of CAM primary tumors.

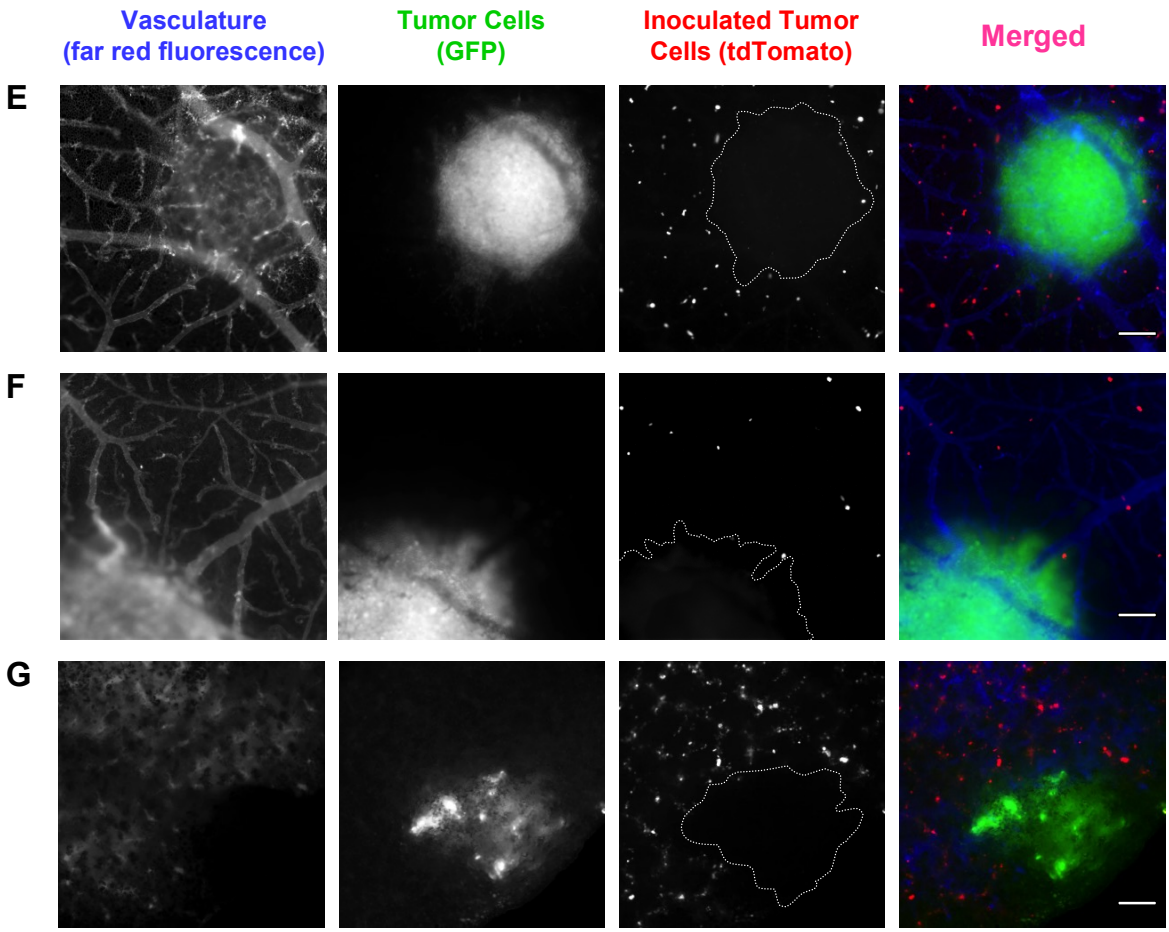

Figure S4 Related to Figure 4 (continued). ***In vivo*** **analysis of intratumoral vasculature for the ability to trap circulating tumor cells.**

(E and F) Intramesodermal tumors were initiated from GFP-tagged HT-hi/diss (**E**) or HEp3 (**F**) tumor cells. Five (HT-hi/diss) and 7 (Hep3) days after cell grafting, tumor-bearing embryos were inoculated with LCA conjugated with far red fluorescence DyLight 649 to stain CAM vasculature (depicted in blue) and human prostate PC-3 carcinoma cells, stably expressing red fluorescence tdTomato protein. 10 min later, primary tumors along with the surrounding CAM tissue were imaged in a fluorescent microscope.

(G) Immunodeficient NOD-SCID mice were grafted into the ear dermis with GFP-tagged HT-hi/diss cells. 2 weeks after cell grafting, primary tumor were resected and mice were allowed to develop lung metastases. 2 month after tumor resection, mice were inoculated i.v. with DyLight 649-conjugated *Lycopersicon esculentum* lectin (Vector Labs) to highlight the vasculature (depicted in blue), followed by

i.v. inoculation of human prostate PC-3 carcinoma cells, tagged with red fluorescence tdTomato protein. Lungs were imaged in a fluorescent microscope 10-20 minutes after tumor cell injections.

In panels **E-G**, images were acquired monochromatically and then "colored" and merged using Adobe Photoshop software. Scale bars, 200 μkm.

The areas of primary tumors (**E and F**) or lung metastasis (**G**) are outlined with dotted lines. Note that these areas are essentially devoid of "red" tumor cells, indicating that intratumoral vessels and vessels within lung metastasis did not "trap" circulating tumor cells.

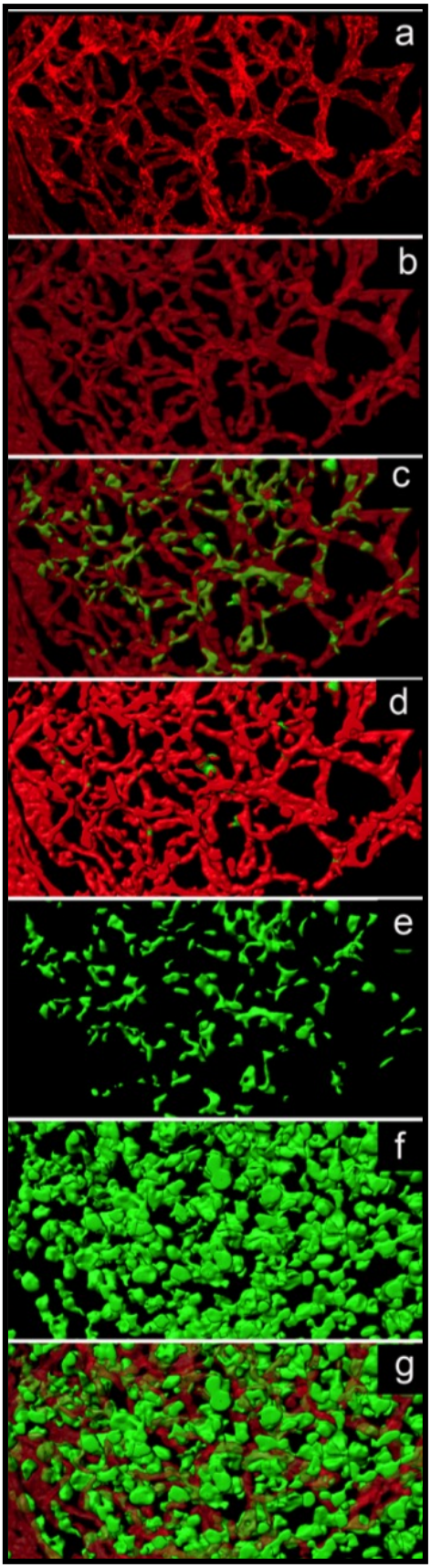

Figure S5 related to Figure 5. <u>Scoring of tumor cell intravasation within the primary tumor by "cell segregation" method</u>.

Figure depicts a sequence of steps conducted within the second, more stringent intravasation-scoring method based on the extraction of the signal associated with tumor cells (*green*) that are fully localized within an isosurfaced and then masked 3D-rendered luminal space of blood vessels (*red*).

(a) Original image of primary tumor portion depicting red fluorescent signal associated with the vasculature;

(b) IMARIS-rendered 3D vasculature isosurfaced twice to fill in (solidify) the available lumen spaces;

(c) IMARIS-rendered mask of tumor cells contained within solidified vasculature in the translucent mode;

(d) The opaque mode of IMARIS-rendered mask of tumor cells within solidified vasculature makes intravasated tumor cells "invisible";

(e) Intravascular tumor cells depicted in (**c**) are presented as a distinct population of tumor cells segregated ("extracted") from the total primary tumor cell population;

(f) IMARIS-rendered total population of tumor cells within the primary tumor region;

(g) IMARIS-rendered total population of tumor cells presented along with translucent vasculature.

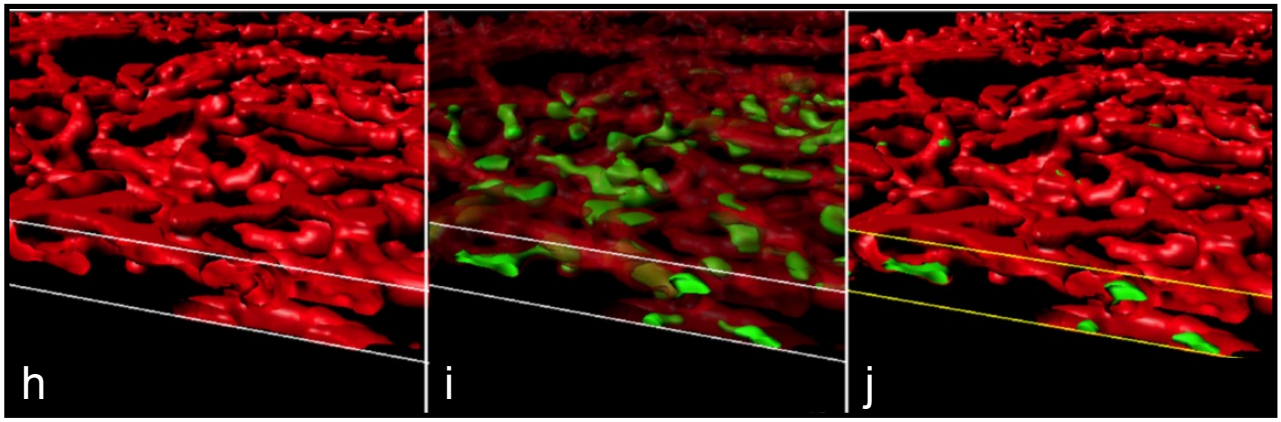

Figure S5 related to Figure 5 (continued). Demonstration of true intraluminal position of the segregated tumor cell population.

Figure confirms that the IMARIS-rendered mask of tumor cell signal "extracted" from the solidified vasculature represents intraluminal tumor cells.

(h) Side view of IMARIS-rendered tumor vasculature, isosurfaced twice (solidified);

(i) IMARIS mask of tumor cells localized within the vasculature (translucent mode);

(j) The slice in the opaque mode that makes tumor cells out of view (invisible). However, intraluminal tumor cells could be seen in the cross section of the slice.

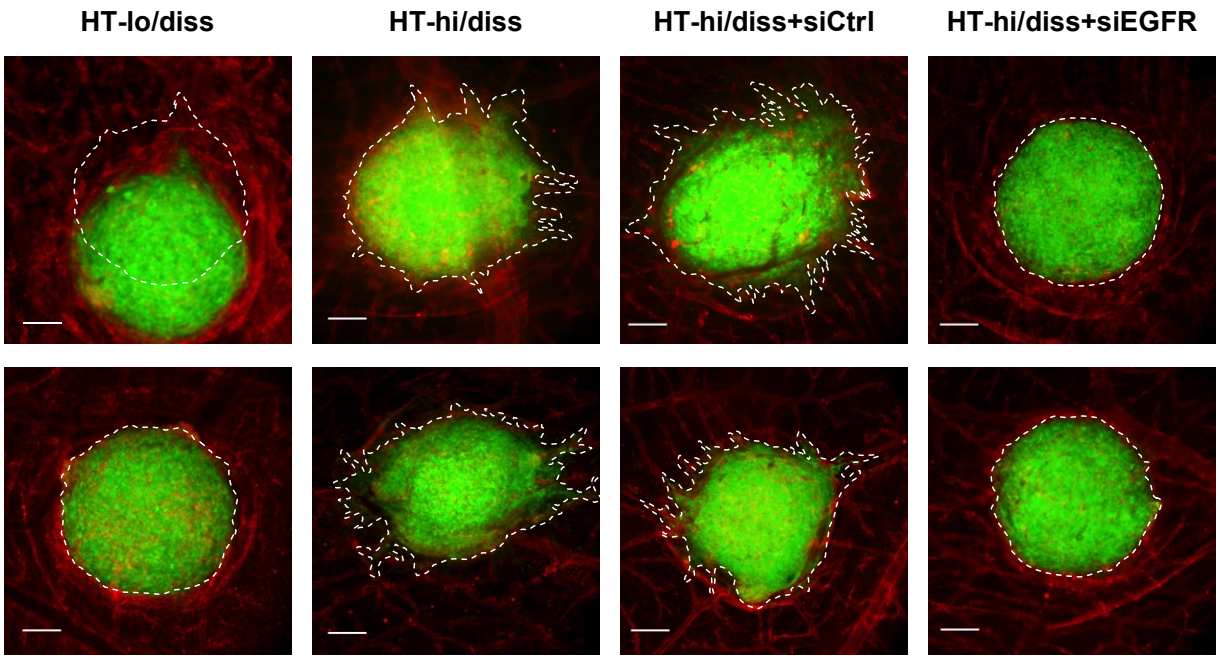

Figure S6 related to Figure 6. Effects of siRNA treatment on HT-1080 primary tumor development.

Figure illustrates the examples of day 5 intramesodermal primary tumors developed after grafting GFP-labeled HT-lo/diss cells and HT-hi/diss cells, the latter were either non-treated or treated with control siRNA (siCtrl) or siRNA against EGFR (siEGFR). Depicted are 2 representative tumors for each cell line and condition. The borders of primary tumors and invasive edges are outlined by dotted lines. Scale bars, 500 μm.

Note that whereas control siCtrl did not affect the overall development of HT-hi/diss tumors, the treatment of cells with siEGFR resulted in the inhibition of invasive front formation and development of largely non-invasive Ht-hi/diss tumors resembling the non-invasive and non-metastatic HT-lo/diss tumors.

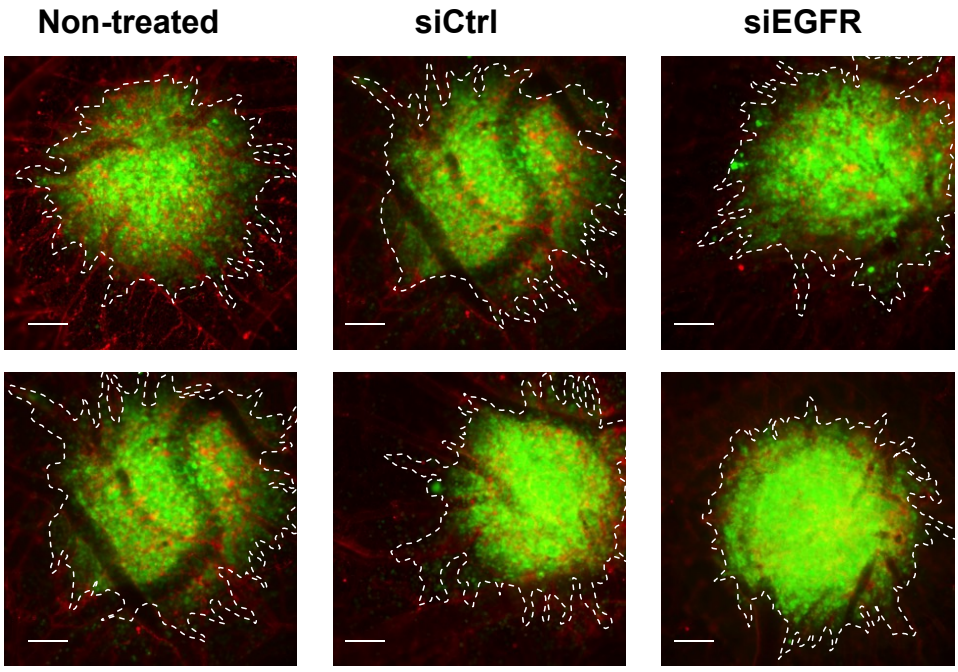

Figure S7 related to Figure 7. Effects of siRNA treatment on HEp3 primary tumor development.

Figure illustrates the examples of day 7 intramesodermal primary tumors developed after grafting of GFP-labeled HEp3 cells, non-treated or treated with either control siRNA (siCtrl) or siRNA against EGFR (siEGFR). Depicted are 2 representative tumors for each condition. The invasive edges of primary tumors are indicated by a dotted line. Scale bars, 200 μm.

Note that control siCtrl did not affect the overall development of HEp3 tumors, which remained invasive, similar to non-treated control. In contrast to EGFR-deficient HT-hi/diss tumors presented in Figure S6, treatment with siEGFR did not substantially reduce the invasiveness of siEGFR-HEp3 tumors compared to siCtrl control.

.

References

Bauer, N., Liu, L., Aleksandrowicz, E., and Herr, I. (2014). Establishment of hypoxia induction in an in vivo animal replacement model for experimental evaluation of pancreatic cancer. Oncology reports *32*, 153-158.

Bekes, E.M., Deryugina, E.I., Kupriyanova, T.A., Zajac, E., Botkjaer, K.A., Andreasen, P.A., and Quigley, J.P. (2011a). Activation of pro-uPA is critical for initial escape from the primary tumor and hematogenous dissemination of human carcinoma cells. Neoplasia *13*, 806-821.

Bekes, E.M., Schweighofer, B., Kupriyanova, T.A., Zajac, E., Ardi, V.C., Quigley, J.P., and Deryugina, E.I. (2011b). Tumor-recruited neutrophils and neutrophil TIMP-free MMP-9 regulate coordinately the levels of tumor angiogenesis and efficiency of malignant cell intravasation. Am J Pathol *179*, 1455-1470.

Conn, E.M., Botkjaer, K.A., Kupriyanova, T.A., Andreasen, P.A., Deryugina, E.I., and Quigley, J.P. (2009). Comparative analysis of metastasis variants derived from human prostate carcinoma cells: roles in intravasation of VEGF-mediated angiogenesis and uPA-mediated invasion. Am J Pathol *175*, 1638-1652.

Deryugina, E.I., Zijlstra, A., Partridge, J.J., Kupriyanova, T.A., Madsen, M.A., Papagiannakopoulos, T., and Quigley, J.P. (2005). Unexpected effect of matrix metalloproteinase down-regulation on vascular intravasation and metastasis of human fibrosarcoma cells selected in vivo for high rates of dissemination. Cancer Res *65*, 10959-10969.

Hirayama, R., Sato, K., Hirokawa, K., Chang, M.P., Mishima, Y., and Makinodan, T. (1984). Different metastatic modes of malignant melanoma implanted in the ear of young and old mice. Cancer Immunol Immunother *18*, 209-214.

Juncker-Jensen, A., Deryugina, E.I., Rimann, I., Zajac, E., Kupriyanova, T.A., Engelholm, L.H., and Quigley, J.P. (2013). Tumor MMP-1 activates endothelial PAR1 to facilitate vascular intravasation and metastatic dissemination. Cancer Res *73*, 4196-4211.

Kim, J., Yu, W., Kovalski, K., and Ossowski, L. (1998). Requirement for specific proteases in cancer cell intravasation as revealed by a novel semiquantitative PCR-based assay. Cell *94*, 353-362.

Li, X.-F., Carlin, S., Urano, M., Russell, J., Ling, C.C., and O'Donoghue, J.A. (2007). Visualization of hypoxia in microscopic tumors by immunofluorescent microscopy. Cancer Research *67*, 7646-7653.

Rademakers, S.E., Lok, J., van der Kogel, A.J., Bussink, J., and Kaanders, J.H.A.M. (2011). Metabolic markers in relation to hypoxia; staining patterns and colocalization of pimonidazole, HIF-1alpha, CAIX, LDH-5, GLUT-1, MCT1 and MCT4. BMC Cancer *11*, 167.

Zijlstra, A., Mellor, R., Panzarella, G., Aimes, R.T., Hooper, J.D., Marchenko, N.D., and Quigley, J.P. (2002). A quantitative analysis of rate-limiting steps in the metastatic cascade using human-specific real-time polymerase chain reaction. Cancer Res *62*, 7083-7092.